Chemical Science

ROYAL SOCIETY OF CHEMISTRY

EDGE ARTICLE

View Article Online
View Journal | View Issue

Cite this: *Chem. Sci.*, 2023, **14**, 8570

All publication charges for this article have been paid for by the Royal Society of Chemistry

Combining native mass spectrometry and lipidomics to uncover specific membrane protein–lipid interactions from natural lipid sources†

Yun Zhu,‡[a] Melanie T. Odenkirk,‡[b] Pei Qiao,‡[a] Tianqi Zhang,[a] Samantha Schrecke,[a] Ming Zhou,[c] Michael T. Marty,[d] Erin S. Baker*[e] and Arthur Laganowsky*[a]

While it is known that lipids play an essential role in regulating membrane protein structure and function, it remains challenging to identify specific protein–lipid interactions. Here, we present an innovative approach that combines native mass spectrometry (MS) and lipidomics to identify lipids retained by membrane proteins from natural lipid extracts. Our results reveal that the bacterial ammonia channel (AmtB) enriches specific cardiolipin (CDL) and phosphatidylethanolamine (PE) from natural headgroup extracts. When the two extracts are mixed, AmtB retains more species, wherein selectivity is tuned to bias headgroup selection. Using a series of natural headgroup extracts, we show TRAAK, a two-pore domain K^+ channel (K2P), retains specific acyl chains that is independent of the headgroup. A brain polar lipid extract was then combined with the K2Ps, TRAAK and TREK2, to understand lipid specificity. More than a hundred lipids demonstrated affinity for each protein, and both channels were found to retain specific fatty acids and lysophospholipids known to stimulate channel activity, even after several column washes. Natural lipid extracts provide the unique opportunity to not only present natural lipid diversity to purified membrane proteins but also identify lipids that may be important for membrane protein structure and function.

Received 21st March 2023
Accepted 19th July 2023

DOI: 10.1039/d3sc01482g

rsc.li/chemical-science

Introduction

Structural and functional studies continue to unveil the crucial roles lipids play in the folding, structure, and function of membrane proteins.[1–7] Several examples include cholesterol having a critical role in promoting the function of the nicotinic acetylcholine receptor from *Torpedo*;[8–10] lactose permease requiring phosphatidylethanolamine (PE) for proper topology and function;[4] the co-purification of KcsA, a pH-regulated potassium channel from the Gram-positive bacterium *Streptomyces lividans*, with a lipid which was later identified to be essential for potassium conductivity;[11] and the requirement of phosphatidylinositol 4,5-bisphosphate ($PI(4,5)P_2$) for activating all inward rectifying potassium channels.[12–16] While these studies highlight the importance of lipids for membrane protein structure, it is challenging to characterize specific membrane protein–lipid interactions and identify lipids important for protein function.

Native or non-denaturing mass spectrometry (MS) has emerged as a powerful way of studying membrane protein–ligand interactions by preserving intact, non-covalent complexes for mass analysis.[1,17–19] It is an indispensable biophysical technique for investigating membrane proteins and their interactions with other molecules, such as lipids.[20] More specifically, native MS over the past decade has revealed that specific protein–lipid interactions can stabilize membrane protein complexes,[1,21,22] allosterically modulate other interactions with proteins,[23,24] lipids,[25] and drugs,[19,26–28] and identify lipids important for function,[1,26–30] such as revealing a new lipid binding site for the ATP-binding cassette transporter MsbA.[31] Another advantage of using native MS to study protein–lipid interactions over other biophysical techniques, such as BRET/FRET-based approaches,[20] is that naturally occurring lipids can be used directly instead of modified forms, such as those conjugated to a fluorophore. To date, most native MS studies have been limited to synthetic lipids due to the structural diversity of natural lipid extracts. Thus, technological developments are warranted to provide insight

[a]*Department of Chemistry, Texas A&M University, College Station, TX 77843, USA. E-mail: alaganowsky@chem.tamu.edu*

[b]*Department of Chemistry, North Carolina State University, Raleigh, NC 27695, USA*

[c]*Verna and Marrs McLean Department of Biochemistry and Molecular Pharmacology, Baylor College of Medicine, Houston, TX, 77030, USA*

[d]*Department of Chemistry and Biochemistry, The University of Arizona, Tucson, AZ 85721, USA*

[e]*Department of Chemistry, University of North Carolina, Chapel Hill, NC 27514, USA. E-mail: erinmsb@unc.edu*

† Electronic supplementary information (ESI) available. See DOI: https://doi.org/10.1039/d3sc01482g

‡ These authors contributed equally to this work.

into lipids from natural sources that bind specifically to membrane proteins.

To date, many lipidomic studies can routinely evaluate around ~500–700 lipids with low false discovery rates. Lipid extraction methods such as the Folch, or Folch-like techniques,[32] rely heavily on releasing lipids into organic solvents. These methods are effective for monitoring the general composition of the lipids but can omit information on protein–lipid interactions. Recently, we illustrated that TRAAK–phosphatidylserine interactions can be modulated by Cu^{2+}, which would be overlooked if studied by lipid extracts alone.[33] Another approach to identifying essential lipids is to extract the membrane protein along with its surrounding lipids, but the co-purified lipids were shown to be dependent on the type of detergent used in the extraction process.[34] Styrene maleic-acid lipid particles (SMALPs) have been used to determine the lipid surrounding multiple proteins in different cell lines.[35–37] However, one downside to copolymers is their low solubility in the presence of divalent ions, which are essential for the activity of many membrane proteins such as ABC transporters.[38,39] However, it is important to note that these methods do not directly report on lipid–protein interactions, making it difficult to ascertain which lipids bind directly to the membrane proteins.

In the past decade, comprehensive lipidomic measurements have been incorporated into other omic evaluations. However, these workflows typically generate singular omic datasets that are integrated into data analysis stages to assess interactions. Here, we combine native MS and lipidomics to characterize lipids that membrane proteins retain from natural lipid sources. More specifically, native MS is performed to measure the masses of lipids bound to the target membrane protein. The lipids are then released for the comprehensive identification of lipids through a multi-dimensional LC-IMS-CID-MS lipidomics method. The integrated approach provides novel opportunities to explore lipid specificity of membrane proteins. Furthermore, it enriches the capabilities of current protein–lipid studies, which often use a subset of synthetic lipids.

Method

Expression constructs

The expression plasmid for AmtB has been previously described and further modified.[40,41] The N-terminal maltose binding protein (MBP) was removed, resulting in an N-terminal secretion signal followed by a TEV protease cleavable N-terminal His_6 affinity tag. The $K_{2P}4.1$ gene (TRAAK, residues 1–295, Uniprot Q9NYG8-2), $K_{2P}10.1$ gene (TREK2, residues 55–335, Uniprot P57789), and Kir3.2 gene (GIRK2, residues 48–378 Uniprot P48051) from *Homo sapiens* were either synthesized as gBlock fragments (Integrated DNA Technologies) or cDNA purchased from DNASU were subcloned into a modified pACE vector (Geneva Biotech), resulting in expression of the target protein with a C-terminal StrepTag II. TRAAK and TREK2 contained N104Q/N108Q and N84Q mutations to remove N-linked glycosylation, respectively. All expression constructs were verified by DNA sequencing.

Protein expression

The AmtB expression plasmid was transformed into *E. coli* C43(DE3) chemical competent cells (Lucigen) by heat shock. The cells with recombinant DNA were inoculated in terrific broth (TB) at 37 °C until the OD_{600} reached 0.6–0.8, and then induced with 0.5 mM IPTG at 25 °C overnight. The recombinant pACEBac1 vectors for TRAAK and TREK2 were transformed into DH10EMBacY chemical competent cells (Geneva Biotech) following the manufacturer's protocol. DH10EmBacY cells successfully incorporated by the recombinant vectors were identified and isolated by white/blue colony screening. Bacmid DNA was purified using HiPure Plasmid Midiprep Kit (Invitrogen), and DNA (30 μg) was mixed with transfection reagent polyethyleneimine (PEI) Max (60 μL, 1 mg mL^{-1}) and PBS (2 ml) before transfecting *Spodoptera frugiperda* (Sf9) cells (30 ml, 0.8 × 10^6 cell per ml, Expression Systems). The transfected Sf9 cells were inoculated at 27 °C for seven days to produce the P1 virus. The P1 virus was clarified with centrifugation (4000*g*, 20 min) under sterile conditions. P1 (5 ml) was used infect *Trichoplusia ni* (Tni) cells (50 ml, 2 × 10^6 cell per ml, Expression system) for protein expression. The infected Tni cells were incubated at 27 °C for two days before harvesting by centrifugation (4000*g* for 20 min at 4 °C).

Purification and delipidation

AmtB. The cell pellet for AmtB was resuspended in lysis buffer A (NaCl 300 mM, Tris 30 mM, pH 7.4) and lysed by three passages through a microfluidizer (M-110 PS, Microfluidics Inc.) operating at 25 000 psi. The cell lysate was clarified by centrifugation at 25 000*g* for 20 min. The supernatant was subjected to ultra-centrifugation (100 000*g*, 2 hours) to harvest the membranes. The membrane pellet containing overexpressed AmtB was resuspended in membrane resuspension buffer RBA (NaCl 150 mM, Tris 50 mM, glycerol 10%, pH 7.4) and homogenized using a glass homogenizer (Wheaton). AmtB was extracted from membranes by the addition of 2% *n*-Dodecyl-β-D-Maltoside (DDM, m/v). The supernatant was clarified by centrifugation (40 000*g*, 20 min), and the supernatant was loaded onto a column containing nickel-charged affinity resin (HisTrap) equilibrated in NHA buffer (RBA with 0.025% DDM and 20 mM imidazole). After sample application, AmtB was washed with 5 column volume (CV) of buffer NHA. Afterward, AmtB was washed with 5CV of NHB buffer (NHA with DDM replaced by 0.5% C_8E_4). Protein was eluted off the column using NHC buffer (NHB with 500 mM imidazole). The eluted AmtB protein was loaded onto a pre-equilibrated HiTrap desalting column (GE) to remove the high-concentration imidazole. The purification and delipidation of TRAAK and TREK2 have been previously described.[33] In brief, Tni cells overexpressing TRAAK and TREK2 proteins were harvested using centrifugation, resuspended, and lysed in KCl-lysis buffer (KCl 200 mM, Tris 50 mM, pH 7.4). The supernatant was centrifuged at 100 000*g* for 2 h at 4 °C. The membrane was resuspended in KCl-lysis buffer and was extracted with 1% DDM at 4 °C for 2 hours. The extracted protein was clarified by centrifugation (20 000*g* for 5 min) followed by syringe filtration (Whatman, 0.45

μm). The filtrate was loaded onto a StrepTrap HP (GE), washed with SPK-DM (KCl 150 mM, Tris 50 mM, glycerol 10%, pH 7.4, 0.2% DM), exchanged into SPK-C10E5 (SPK with 0.062% $C_{10}E_5$), and eluted with SPK-C10E5-DTB (SPK-C10E5 with 3 mM D-desthiobiotin). Similar to TRAAK, TREK2 was lysed and extracted in KCl-lysis buffer with 1% OGNG (2,2-dihexylpropane-1,3-bis-β-D-glucopyranoside), purified with SPK-OGNG (SPK with 0.12% OGNG) and SPK-OGNG-DTB (supplemented with 3 mM D-desthiobiotin). The purified TREK2 protein was treated with Endo H (New England Biolabs) overnight at 4 °C to reduce glycan heterogeneity. Afterward, TREK2 was repurified on a StrepTrap HP to remove glycans and buffer exchanged into SPK-C10E5. Both TRAAK and TREK2 were desalted using a HiPrep 26/10 Desalting column (GE).

Washing and preferential retention of lipids from extracts

Lipid extracts were purchased from Avanti Polar Lipid (Table S1†) and prepared as previously described.[42] In brief, dried lipid films were rehydrated in MilliQ water to desired concentrations. For lipid wash studies of AmtB, *E. coli* AmtB (1 μM) was incubated with either phosphatidylethanolamine (EcPE, 10 mg ml^{-1}), *E. coli* cardiolipin (EcCDL, 10 mg ml^{-1}) or a 1 : 1 mixture of the two extracts at room temperature for 1 hour. The protein–lipid mixture was then loaded onto a HisTrap pre-equilibrated in NHB and washed with NHC. AmtB protein was eluted with NHC. For lipid headgroup extracts affinity experiments with TRAAK (2.2 μM), the method was modified to include the addition of the lipid headgroup extract after 2 column volume (CV) washes. Two additional washes were used to elute any non-preferential lipid binding. TRAAK (2.2 μM) and TREK2 (2.2 μM) were individually incubated with brain extract polar lipid (BEP) (1.2 mg ml^{-1}) for 0.5 h before loaded onto a in-house prepared strep-column (~200 μL bed volume, Strep-Tactin sepharose resin, iba). Immobilized lipid-protein complexes were washed with SPK-C10E5 for desired amount of CV washes and were eluted with SPK-C10E5-DTB. Similar experiments were conducted for headgroup extracts. All lipid extracts were selected as a proof of concept to demonstrate the ability of native MS and lipidomics to define protein–lipid interactions in complex lipid environments.

Native MS

Membrane protein samples were buffer-exchanged into aqueous ammonium acetate (200 mM, pH 7.4 adjusted with ammonium hydroxide) supplemented with 0.5% C_8E4 (AA C_8E_4) for AmtB or 0.065% $C_{10}E_5$ (AA $C_{10}E_5$) for the other proteins using a centrifugal desalting column (Micro Bio-Spin 6, Bio-Rad). The protein–lipid mixtures were loaded into a gold-coated glass emitter (prepared in-house) and introduced into a Q Exactive UHMR Hybrid Quadrupole-Orbitrap mass spectrometer (Thermo). The instrument parameters were set as follows: For AmtB, capillary voltage of 1.50 kV; capillary temperature of 200 °C; Collision-Induced Dissociation (CID) of 50 V; Collision Energy (CE) of 80 V; trapping gas pressure setting to 3.0; source DC offset of 20 V; injection flatapole DC of 10 V; inter flatapole lens of 6 V; Bent flatapole DC of 4 V; transfer multipole DC of 6 V. For TRAAK and TREK2, capillary voltage of 1.50 kV; capillary temperature set to 300 °C; CID of 50 V; CE of 50 V; trapping gas pressure set to 5.0; source DC offset of 40 V; injection flatapole DC of 8 V; inter flatapole lens of 4 V; bent flatapole DC of 3 V; transfer multipole DC of 3 V. The MS data collected from native MS were deconvoluted using UniDec and Protein Metric software.[43,44] Mass error was determined for the bound lipids based on the center of each peak.[45]

Lipidomics

The comprehensive identification of retained lipids from membrane protein samples was completed on an Agilent 1290 Infinity II UHPLC (Santa Clara, CA) coupled to an Agilent 6560 IM-QTOF MS platform (Santa Clara, CA) following a 1 : 100 sample dilution in methanol. 10 μL injections of each sample were initially separated at a flow rate of 250 μL min^{-1} on a reversed-phase Waters CSH column (3.0 mm × 150 mm × 1.7 μm particle size). The 34 minute gradient (MPA : ACN/H_2O (40 : 60) with 10 mM NH_4Ac and MPB : ACN/IPA (10 : 90) with 10 mM NH_4Ac) and subsequent 4 minute wash and re-equilibration steps are detailed in Tables S2 and S3 in the ESI.† For anionic lipid class extracts including PE, CDL, PG, and PS, IMS-MS data was collected solely with negative ESI from 50 to 1700 *m*/*z*. BEP and PC lipid extracts were conversely measured across the same mass window in both positive and negative ionization modes. MS operation also included an alternating scan method of no fragmentation (MS1) and all-ions data-independent acquisition (DIA) to simultaneously capture MS and MS/MS spectra. To optimize fragmentation across complex samples, a ramped collision-induced dissociation (CID) method was employed based on IMS drift times.[46,47] Additionally, all analyses were conducted with a cycle time of 1 s per spectra to enhance the low abundant ion signal.

Skyline was used to deconvolve spectra and assign lipid identifications for the multidimensional LC-IMS-CID-MS lipidomic analysis conducted herein.[48–50] For brain lipid extract samples, an in-house library of 623 lipids with experimentally validated LC, IMS, and MS information was used to assign all identifications.[48,51,52] For class-based extracts, LipidCreator was used to enumerate all the potential identifications for 2-tailed lipids and lysolipids that contained fatty acyls with a length between 12-22 carbons and 0–6 double bonds.[53] These libraries were then uploaded into Skyline to first identify precursor mass matches with ≤5 ppm mass error for representative isomers. Alignment of computational collision cross-section and retention times was subsequently used to assign the correct fatty acyl composition for all precursor matches.[52] The resulting speciation of identifications typically included both head group and fatty acyl assignments (*i.e.* PE(16 : 0_18 : 1)) except for cardiolipins and other lipids with ambiguous fatty acyl assignments that were instead reported with summed fatty acyl composition (*i.e.* CL(70 : 3)). Precursor peak areas of all identified lipids were normalized to the total ion current and log_2 transformed. Transformed data of each sample is presented in ESI Tables S4–S10.† For inquiries into natural lipid preference across membrane protein experiments, comparisons were

completed through a qualitative analysis of lipid identifications unless otherwise noted. For visualization of fatty acyl trends across head groups, an additional normalization to the analyte with the highest signal within each class was also completed. Membrane-protein lipid affinities were visually assessed for both head group and fatty acyl trends with various components of the Structural-based Connectivity Omic Phenotype Evaluations (SCOPE) cheminformatics toolbox.[54] Additional enrichment analysis of lipid species was completed with Lipid Mini-on.[55]

Results

Overview of the approach

As natural products have been exploited to identify small molecules for drug discovery,[56] we set out to develop a new method to identify specific membrane protein–lipid interactions retained from various natural lipid sources (Fig. 1), such as a brain polar lipid extract or natural headgroup extracts. This method uniquely combines native mass spectrometry with lipidomics to probe both the protein and lipid components. To begin, the target membrane protein sample should be devoid of major co-purified contaminants, such as co-purified lipids, which can be confirmed by a native mass measurement (ESI Fig. 1†). Co-purified contaminants may inadvertently influence the preference of lipids from natural extracts, so their absence is essential. The target membrane protein solubilized in detergent is then mixed and incubated with a natural lipid extract (Fig. 1a). This mixture is applied to a drip column containing affinity resin to capture the tagged, target membrane protein (Fig. 1b). For example, a membrane protein can be fused to a poly histidine sequence, typically six in total, to enable purification of the affinity tagged protein using immobilized metal affinity chromatography and subsequently eluted using imidazole (see Methods for details). The immobilized target protein is washed with different column volumes of buffer containing detergent (Fig. 1c), thereby washing away loosely associated lipids. Multiple drip columns can be used in parallel to obtain different column volume washes in one step. The eluted protein–lipid samples are then buffer exchanged into ammonium acetate with detergent at two times the critical micelle concentration (2× CMC) for native MS studies (Fig. 1d). Native mass spectra are then recorded to provide a direct measurement of the associated lipids and their masses (Fig. 1e). Orthogonally, the same sample is also subjected to lipidomic analyses (Fig. 1f) to identify lipids that bind to the target protein. Furthermore, the lipid masses from the native MS studies aid in filtering the lipids identified in the lipidomic studies (Fig. 1g). This represents the unique aspect of our method, wherein lipid binding to the protein is confirmed (native MS) and each lipid is comprehensively identified (lipidomics).

PE modulates AmtB–CDL interactions

Since interactions of the bacterial ammonia channel (AmtB) with cardiolipin (CDL) are known to be enhanced in the presence of phosphoethanolamine (PE),[25] we used this system in our first analysis. The native mass measurements of apo AmtB revealed the pelB secretion signal was cleaved at two positions, resulting in different masses of the trimeric complex (ESI Fig. S1†). While this complicates the mass spectrum, it does not

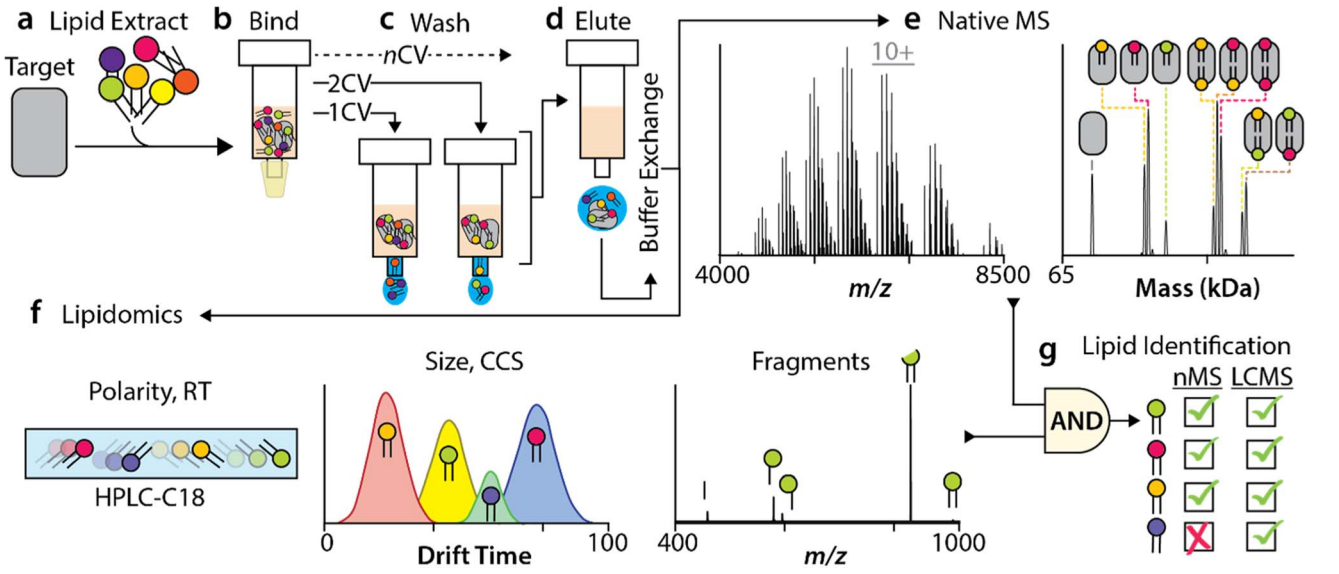

Fig. 1 Overview of the method to identify lipids enriched by an immobilized target membrane protein from natural lipid extracts. (a) The target membrane protein is first incubated with a natural lipid extract followed by (b) loading onto different, pre-equilibrated affinity columns. The immobilized protein–lipid complexes are (c) washed with different column volumes (CV) of the detergent-containing buffer. After a given number of washes, the (d) eluted protein–lipid complexes are buffer exchanged into 200 mM ammonium acetate and (e) analyzed by native mass spectrometry to determine the masses of lipids bound to the target protein. The same samples used for native MS studies are (f) subjected to lipidomic analyses, cataloguing the enriched lipids. (g) The masses determined from native MS are used to filter the lipids identified in lipidomics, pinning down the most tightly-associated lipids.

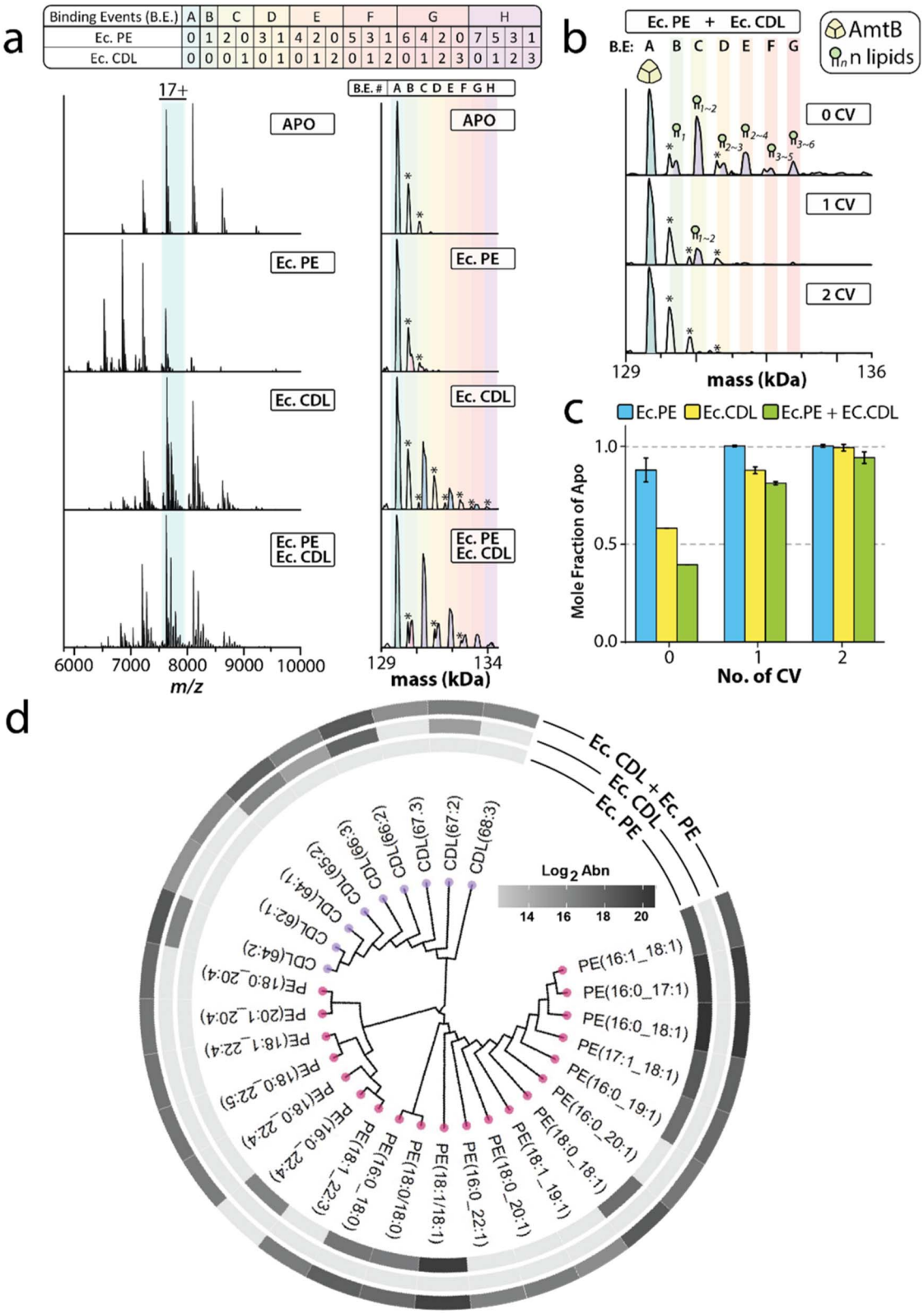

Fig. 2 The ammonia channel (AmtB) enriches specific lipids from *E. coli* PE and CDL extracts. (a) Representative mass spectra (left) and zero charge spectra (right) of AmtB and mixed with *E. coli* PE extract, *E. coli* CDL extract, and a mixture of the two headgroup extracts. The secretion signal of AmtB was found to be processed at two locations, giving rise to different masses for apo AmtB and denoted by an asterisk. (b) Deconvoluted mass spectra of AmtB incubated with a mixture of *E. coli* PE and CDL extracts followed by 0 to 2 CV wash with detergent-containing buffer. (c) Plot of the mole fraction of apo AmtB for incubation in different lipid extracts and washed with 0 to 2 CV of the buffer. The presence of the PE extract enhances the enrichment of CDL species. (d) Lipidomic analyses of lipids enriched from *E. coli* PE extract, *E. coli* CDL extract, and a mixture of the two bacterial headgroup extracts.

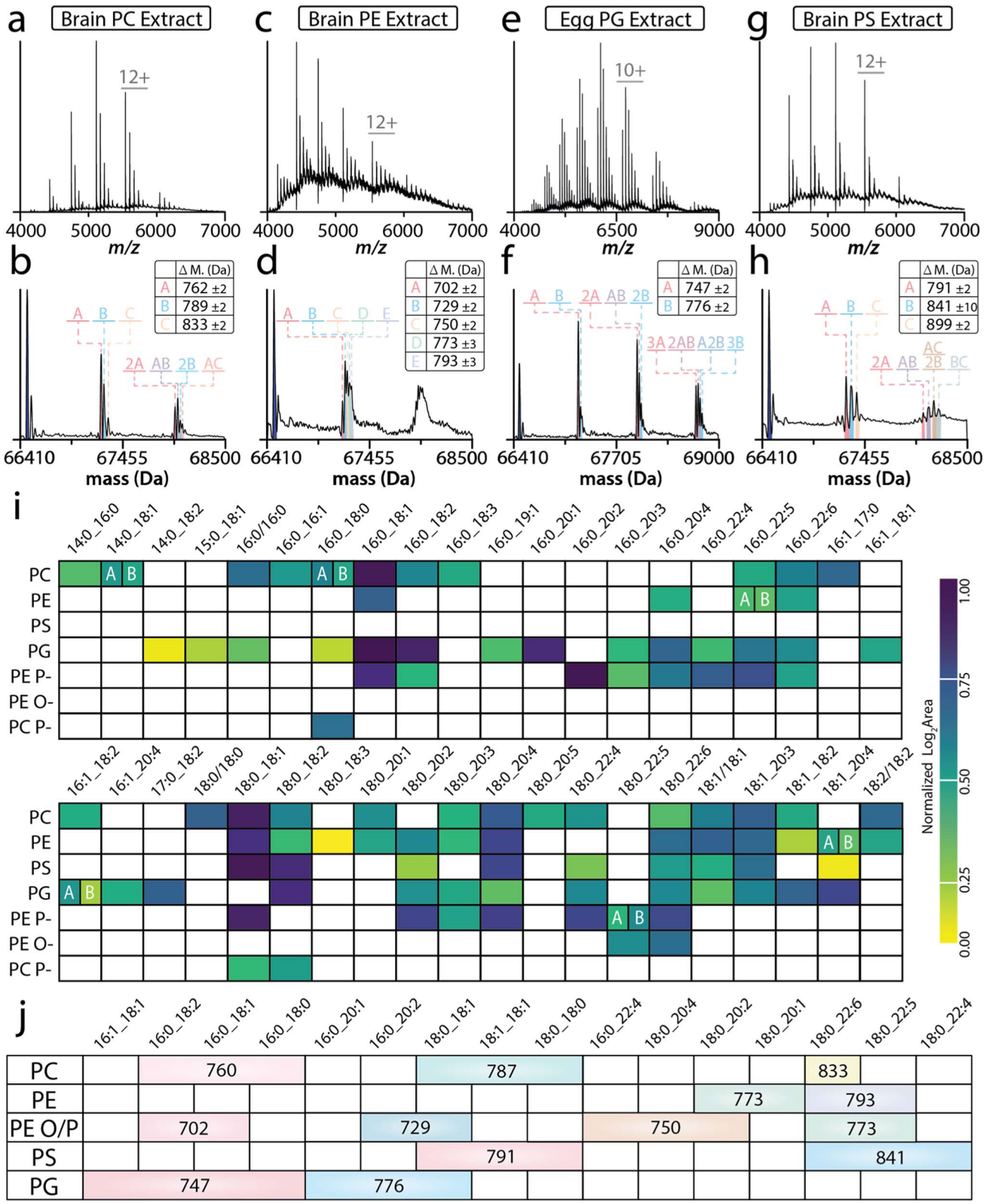

Fig. 3 TRAAK selectively enriches lipids with distinct acyl chains from natural headgroup extracts. (A) Representative native mass spectrum of TRAAK incubated with (a) brain PC extract and (b) deconvolution, (c) brain PE extract and (d) deconvolution, (e) egg PG extract and (f) deconvolution, or (g) brain PS extract and (h) deconvolution followed by 2 CV wash. The deconvoluted mass spectrum is shown underneath with adduct masses annotated. (i) Heatmap of lipid identifications from the lipidomic analyses of each lipid class extract (rows) and their corresponding fatty acyl content (columns). Empty cells represent undetected pairs while the colored heatmap reflects the normalized abundance of an individual lipid identification (*i.e.* the top corner box of PC(14 : 0_16 : 0)). This visualization reveals different lipid species retained from lipid headgroup extracts. (j) Native mass measurements filter results from lipidomics to identify specifically retained lipids. Abbreviations are listed in Table S1.†

preclude us from characterizing protein–lipid interactions. AmtB mixed with an *E. coli* CDL extract (EcCDL) followed by 1 CV wash shows up to 3 lipids bound (Fig. 2a). Application of 3 CV wash removes the majority of bound EcCDL species from AmtB. However, AmtB holds onto EcCDL with a mass of 1373 ± 60 Da. Similar observations were made for the *E. coli* PE extract (EcPE). Up to 2 bound lipids were observed for EcPE when the mixture of AmtB and EcPE was treated with 1 CV wash. EcPE species with a mass of 757 ± 55 Da were bound to AmtB after the application of a 2 CV wash.

Interestingly, incubation with a mixture of both headgroup extracts enhanced the retention of both lipid extracts, which was more pronounced for EcCDL (Fig. 2b and c). The lipidomic analysis also showed the preference of more EcPE and EcCDL species (Fig. 2d and Table S4†), consistent with the native MS results that illustrated the broadening of the mass spectral peaks (Fig. 2b). Interestingly, 10 PE species and 5 CDL species were retained from the incubation of each respective extract with AmtB. The mixture however exhibited nearly double the number of identified lipids for each class (19 PE and 10 CDL) to a total of 29 species. In the extract mixture, the new lipid species AmtB retained were two CDL species (62 : 1 and 64 : 1 CDL) and two tri-unsaturated species (67 : 3 and 68 : 3 CDL). For the PE species, AmtB retained 9 new species that all contained at least one fatty acyl chain with a length ≥20, and one double bond. Notably, five of these lipids contained a polyunsaturated-fatty acyl (PUFA) chain (Table S4†). Distinctly, PE (16 : 0_22 : 4) is detected when EcPE is used alone but absent when the mixed extract is used. In short, PE modulation of AmtB–CDL interactions results in the enhancement of headgroup recognition but not acyl chain selectivity (Fig. 2d).

TRAAK and lipid headgroup extracts

Next, we focused on the use of natural headgroup extracts to investigate whether specific acyl chains can be retained. TRAAK is a mammalian two-pore domain potassium channel known to be modulated by lipids, such as stimulated by Arachidonic Acid as illustrated by the AA in TRAAK,[57] and expressed predominantly in the central and peripheral nervous system.[58,59] TRAAK was incubated with different natural headgroup lipid extracts: brain PC extract, brain PE extract, egg PG extract, and brain PS extract. After a 2 CV wash, TRAAK retained three lipids from the PC extract with masses of 760 ± 2, 787 ± 2, and 833 ± 2 Da (Fig. 3a and b). TRAAK contains a C-terminal strep-tag, which can affinity purified using immobilized Strep-Tactin.[60] For the two-ligand bound state, masses corresponding to different combinations of the three PC lipids are observed (Fig. 3b). For the brain PE extract, TRAAK retained more than 5 PE species (702 ± 2, 729 ± 2, 750 ± 2, 773 ± 3, and 793 ± 3 Da) that could be assigned for the 1st lipid-bound state. The mass spectral peak of subsequent binding events was too broad to assign masses for distinct PE combinations (Fig. 3c and d and ESI S2c and d†). For the PG extract, the first bound lipid was predominated by two species (747 ± 2 Da and 776 ± 3 Da), and subsequent binding events resulted in broad mass spectral peaks inhibiting the ability to assign masses. A weak signal was also observed for two lipids with masses of 795 Da and 820 Da (ESI Fig. S2f†). Lastly, TRAAK retained three major species from the PS extract: 791 ± 2 Da, 841 ± 10 Da, and 899 ± 2 Da (Fig. 3g and h). Additional studies illustrated that the 841 Da peak was the result of two overlapping peaks, which could be resolved when the data was acquired using a higher mass resolution setting on the instrument (Fig. S2h†). The peak splitting is due to the binding of Cu^{2+}, which we have recently shown specifically modulates TRAAK–PS interactions.[33] In short, these results illustrate that TRAAK retains distinct masses from the natural headgroup extracts.

Native MS alone provides a mass accuracy that reflects a broad window of potential bound lipid species. For example, the 760 ± 2 Da window defined by the native MS analysis of TRAAK mixed with a PC lipid extract matches a total of 98 unique PC lipids in the LipidMaps database for this mass tolerance.[61] These 98 potential identifications reflect lipids identified at the head group and individual fatty acyl level with no information on double bond position or geometry and *sn*-positioning. Therefore, ambiguity lies in the annotation of lipids from native MS alone. Conversely, comprehensive lipidomics requires a sacrifice of local molecular interactions to provide detailed lipid speciation and holistic coverage of lipidome composition. To provide further lipid identification following the discovery of TRAAK enriching specific lipids from various headgroup extracts, a comprehensive LC-IMS-CID-MS lipidomic analysis was used to further speciate bound lipids based on mass additions observed in native MS experiments. For the PC extract, we identified a total of 32 lipid species and reduced the 760 ± 2 Da lipid pool from native MS to three potential lipids: PC(16 : 0_18 : 2), PC(16 : 0_18 : 1), and PC(16 : 0_18 : 0), highlighting the complementarity of these two techniques and significantly reducing the number of potential lipid candidates for additional follow-up experiments. The remaining 788 ± 2 Da adduct includes both PC(18 : 0_18 : 1) and PC(18 : 1/18 : 1) as potential bound lipid candidates (Fig. 3i and Table S5†). The largest PC species (833 ± 2 Da) was mapped to PC(18 : 0_22 : 6), however, it is also plausible this species could also be a 787 ± 2 Da lipid with a K^+ adduct (ESI Fig. S2a and b†).

Native MS of the PE extract exhibited 5 bound lipid masses. Notably, plasmalogen lipids were the only lipids identified in the mass windows derived from native MS. The 747 ± 2 Da PG matched two potential lipids, PG(16 : 0_18 : 1) and PG(16 : 0_18 : 2), whereas the 776 ± 3 Da species matched three lipid isomers (PG(16 : 0_20 : 1), PG(18 : 0_18 : 2) and PG(18 : 1/18 : 1)) that were distinguishable from our lipidomics analysis (Fig. 3e, f and Table S7†). For the PS extract, the 791 ± 2 Da is assigned as matching PS(18 : 1/18 : 1), PS(18 : 0_18 : 1), and PS(18 : 0/18 : 0). The final 841 ± 10 Da species corresponds to PS(18 : 0_22 : 6), PS(18 : 0_22 : 5), and PS(18 : 0_22 : 4). We also note the relative intensity of each adduct is like those detected in the natural lipid extracts (ESI Fig. S2 and S3†). Notably, many of the retained lipid species identified by lipidomic analysis matched the masses measured for the lipids bound to TRAAK deduced from native MS measurements (Fig. 3i).

Next, we sought to elucidate global trends of TRAAK's affinity for specific lipids. To facilitate the visualization of fatty acyl

trends across the various head group class extracts investigated here, we employed the SCOPE cheminformatics toolbox to create a heatmap of normalized lipid abundance for all unique fatty acyl combinations across each lipid class extract (Fig. 3j).[54] This allowed us to explore general trends for all the identified lipids across each class. Here, we noted several re-occurring fatty acyl motifs across lipid classes. This included a heightened preference for 16 : 0_18 : 1 and 18 : 0_18 : 1 lipid species within each class extract. The only exceptions to this were longer-chain PUFA-containing lipids and alkyl/alkenyl ether (O/P) lipids detected in the PC and PE lipid extracts. Globally, we also noted that of the identified species, TRAAK showed preference for PUFA-containing lipids, specifically when their counterpart was an 18 : 0 or 18 : 1 acyl chain. In our previous study using synthetic lipids, TRAAK–lipid interactions showed a preference toward the acyl chain chemistry, as well as the *sn1* fatty acid linkage.[42] While these *sn* isomers cannot be definitively annotated on the lipidomic analysis platform leveraged here, the separation of these species by chromatography is plausible. Here, we observed four lipid isomers pairs (denoted A

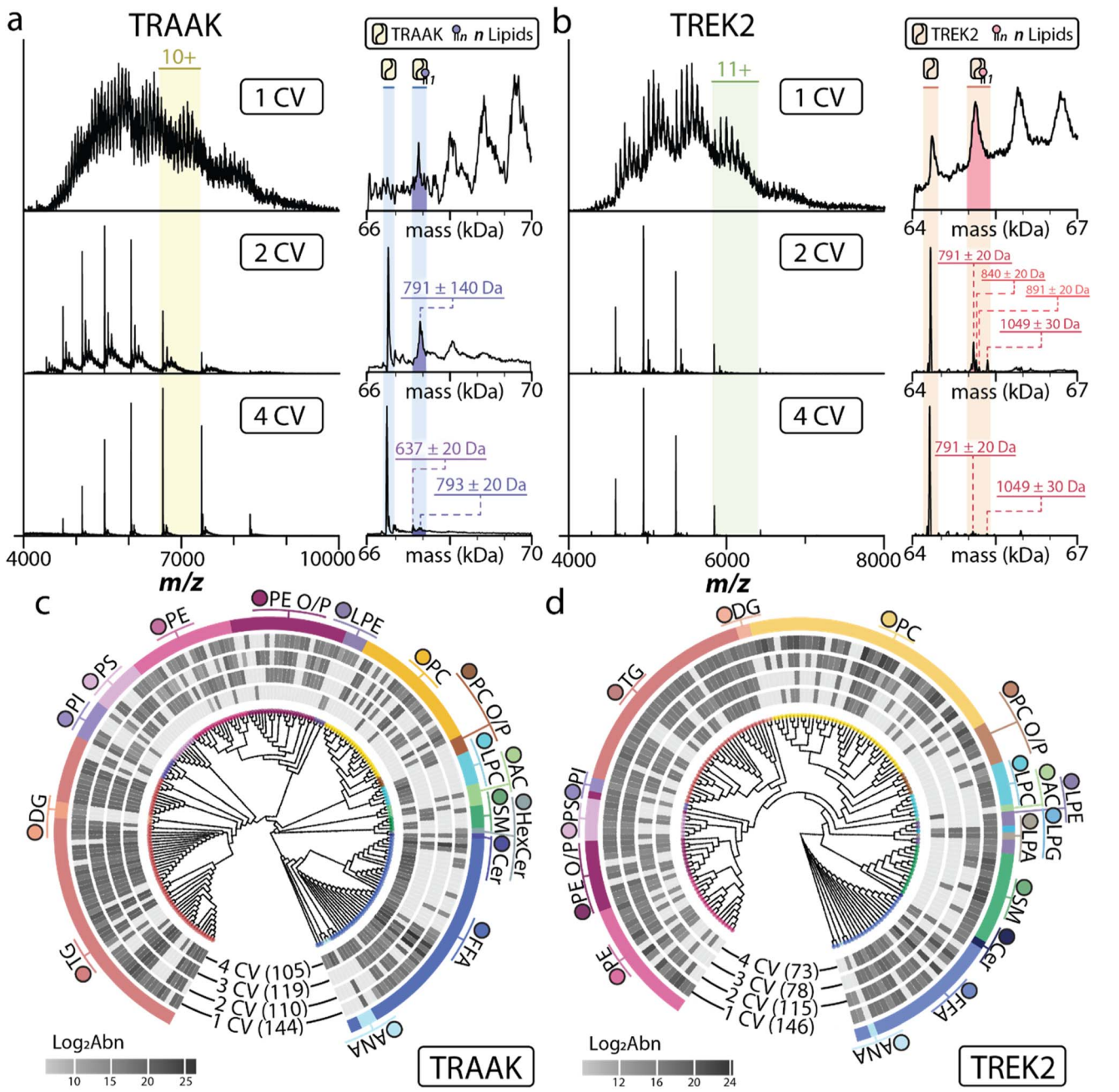

Fig. 4 Selective enrichment of lipids from a brain polar lipid extract using immobilized TRAAK and TREK2. (a and b) Native mass spectrum of (a) TRAAK or (b) TREK2 incubated with brain polar extract followed by different CV washes. The deconvoluted mass spectra are shown to the right. (c and d) Lipidomic analyses of lipids retained from a brain polar extract by (c) TRAAK and (d) TREK2. The different CV washes are labeled. Abbreviations are listed in Table S1.† Full lipid identifications and log 2 area values are presented in Tables S9 and S10.†

and B) across class extracts. Notably, isobars PC(14 : 0_18 : 1); PC(16 : 0_16 : 1) and PE(16 : 0_22 : 5); PE(18 : 1_20 : 4) showed relatively similar responses, while A and B isomers of PG(16 : 1_18 : 2) and PE(P-18 : 0/22 : 5) showed differing relative abundance. Taken together, these results demonstrate that TRAAK retains lipids with specific acyl chains independent of the headgroup.

TRAAK and TREK2 lipid affinities in natural mammalian extracts

Moving beyond natural headgroup extracts, we investigated whether membrane proteins would retain specific lipids from a brain polar lipid extract (BEP). For these studies, we used TRAAK and TREK2, a K2P that shares ~45% sequence identity with TRAAK.[57,62] Again, both channels were incubated with BEP and underwent multiple CV washes to elute lipids with various affinities. For both channels, the native mass spectra showed that most lipids were washed away after 2 CV washes, and nearly all adducts were removed after 4 CVs (Fig. 4a and b). A group of adducts centered around 791 Da was detected for the first lipid-bound state of TRAAK after a 2 CV wash. However, higher lipid-bound states were more heterogeneous, hindering the accurate assignment of adduct masses (Fig. 4a and ESI Fig. S4a and b†). After a 4 CV wash of immobilized TRAAK, the underlying broadness was decreased as well as the adduct signals. This allowed for some adduct masses to be assigned (637 Da, 677 Da, 752 Da, 793 Da, 838 Da, and 886 Da). Interestingly, the 791 Da species were retained after 2 and 4 CV washes (ESI Fig. S4a and b†). The 677 Da retained by TRAAK after 4 CV wash is consistent with the mass of PA(16 : 0_18 : 1), a lipid that binds tightly to TRAAK.[42]

In contrast, TREK2 displayed more defined peaks after 2 CV washes (Fig. 4b and ESI Fig. S4e and f†). Like TRAAK, most of the retained lipids were depleted from TREK2 after the application of a 4 CV wash. Masses could be determined for many lipid-bound states of TREK2 (729 Da, 753 Da, 790 Da, 838 Da, 891, and 1047 Da). TREK2 also retained a species of 1048 Da that is consistent with phosphorylated phosphatidylinositol, which is known to regulate TREK2.[63,64] However, this lipid was not observed in the lipidomic analysis. Interestingly, both channels retained a subset of lipids with similar masses and at a relatively similar ratio. These results demonstrate that immobilized membrane proteins can enrich specific lipids from a complex lipid extract, such as BEP.

To provide a holistic view of TRAAK and TREK2 lipid enrichment, we also performed a comprehensive lipidomic analysis. The resulting identifications were assessed based on structural motifs to further characterize the lipid environment changes for each CV wash.[55] In the analysis of CV washes for TRAAK and TREK2, a total of 206 and 165 lipids were identified across 16 and 19 lipid classes (Fig. 4c and d). Globally, lipidomic analysis of subsequent CV washes for both potassium channels showed a decrease in the number of unique identifications while also displaying unique lipid affinities. For TRAAK, the wash profile for 1 CV initially included 148 species, largely across triacylglycerols (TGs), phospholipids, and free fatty acids (FFAs). With each wash step, we observed a decrease in the number of lipid signals except for 3 CVs, where an influx of diacyl phospholipid species specifically within PI lipids occurred and the total number of identified lipids slightly increased from 110 to 119 identifications. In the final wash step, a significant number of FFA species in addition to lyso PC (LPC) and PE lipids were observed. This final wash also contained a surprising amount of TG signal and few diacyl phospholipid species (Table S9†).

Like TRAAK, the 1 CV lipid profile of TREK2 contained lipids across TGs, phospholipids, and FFAs in addition to a heightened presence of SM species. As the number of washes increased, a significant amount of anionic phospholipid signal was retained. Contrasting the TRAAK profiles, LPC and PE species were only observed in the 1 CV wash for TREK2. Additionally, we observed signal for lyso-PG (LPG) and lyso-PA (LPA) species that remained present across all wash steps. To further survey lipid associations of TRAAK and TREK2, enrichment analysis of lipid ontology for all wash steps was conducted relative to the lipid library queried in this study. This allowed us to ascertain several additional associations of lipids with shared structural motifs to either membrane protein. Namely, TRAAK, PS, and PE lipids were uniquely enriched in 2 CV and 4 CV washes. FFAs were also enriched in the first and last CV wash steps. We also observed an enrichment of lipids with saturated fatty acids in 2 CV and 4 CV with 18:0-containing lipids being uniquely enriched in the last wash step. Interestingly, PUFAs were enriched by TRAAK after a 4 CV wash. Conversely, enrichment analysis for TREK2 washes favored fatty acyl content, including enrichment of several 20:4-containing diacyl species after 1 and 2-column washes and PS class enrichment. In subsequent washes, this trend was later reversed, showing predominantly saturated fatty acids and enrichment of TG and FFA classes. A table of all enriched structural motifs is presented in Tables S9 and S10.† Data has been deposited at Panorama and can accessed at **https://doi.org/10.6069/ermp-tp39**.

Discussion

Previous work has shown AmtB interactions with TOCDL (all 18 : 1 tails) are allosterically modulated in the presence of PE(16 : 0/18 : 1),[25] which is recapitulated here using EcPE and EcCDL extracts. The global lipidomic analysis shows that AmtB presented with an EcPE and EcCDL mixture retains nearly two-fold more lipid species when compared to the individual class extracts. The additional PE lipids identified contained poly- and mono-unsaturated fatty acyl chains. A notable exception was PE(16 : 0_22 : 4), which was only observed in the EcPE extract, indicating AmtB is also selective to acyl chains of PE. Like PE, we identified double the number of cardiolipin species compared to the EcCDL extract alone. This included two monosaturated and two tri-saturated species. Interestingly, the lipids that were exclusively retained from the lipid extract mixture corresponded to those containing one or more unsaturated bonds. The presence of double bonds and their stereochemistry can influence membrane fluidity.[65,66] While AmtB-PE

interactions have previously been shown to be rather non-selective, AmtB in the presence of both EcPE and EcCDL results in increased binding to both of these lipids. This enhancement is the result of altering the selectivity toward the headgroup at the cost of acyl chain preference. Taken together, these results demonstrate a lipid can enhance specific membrane protein–lipid interactions by tuning the selectivity toward the headgroup, which will result in enhanced lipid binding as observed for the EcPE and EcCDL mixture. This also suggests the opposite could occur, that is specific membrane protein–lipid interactions can be tuned by altering the selectivity to the acyl chains of the specific lipid.

An important question to address is how acyl chain chemistry influences membrane protein–lipid interactions. Different headgroup extracts (PC, PE, PG, PS) show TRAAK retains specific acyl chains within each class. Previous work characterizing TRAAK binding synthetic lipids containing 1-palmitoyl-2-oleoyl (16 : 0_18 : 1, PO) acyl chains illustrated POPS to be the weakest binder among the headgroups investigated.[67] The PS extract had the lowest number of identifications (10 in total), a result consistent with the low affinity of TRAAK for POPS. Interestingly, the PS species identified contained long acyl chains (≥18). For the remaining lipid classes, lipids containing either 16 : 0 or 18 : 0 and one PUFA were predominant among the different head groups. Previous work has shown TRAAK has a stronger preference for PE and PA lipids, and binding affinity can be highly variable and also dependent on the headgroup.[42] Examples of this include the anticipated lipid binding across each class observed from native MS measurements. For example, we observed that 16 : 0_18 : 1 and 18 : 0_18 : 1 containing lipids were abundant across multiple lipid classes. While the use of synthetic lipids can be informative, our approach has identified new acyl chain preferences for TRAAK. In addition, the preference for specific acyl chains was not dependent on the headgroup. In short, natural headgroup extracts provide the unique opportunity to display varied acyl chain chemistry to better understand requirements that underly specific membrane protein–lipid binding sites.

Following the observed allosteric effects for AmtB–lipid interactions and the identification of acyl chain preferences for TRAAK, we next sought to explore if select membrane proteins TRAAK and TREK2 would retain species from mammalian lipid extracts.[68] To further understand the affinities of each protein for selecting lipids, four serial wash steps were used to remove lipids sequentially, *i.e.* washing away the weakly binding lipids. Native MS provided some insight into the masses for the first lipid however subsequent binding events displayed broad distributions. These results indicate that TRAAK and TREK2 can retain a subset of lipids from the complex brain polar extract. To identify the retained lipids, our analysis first considered the global profile of lipids observed relative to an established library developed in-house for identifying lipids in LC-IMS-CID-MS data.[50,51] Overall, a total of 206 and 165 identifications were made from the library consisting of 623 lipids for TRAAK and TREK2.[48] As was anticipated with subsequent wash steps, a gradual decline in the number of lipid identifications was observed. This result demonstrates the approach can be useful in identifying lipids that readily associate with the target membrane protein.

Here, TRAAK and TREK2 initially contained 146 and 118 lipids in the first CV wash and then 105 and 73 lipids in the four-column wash step. These profiles were then subjected to enrichment analysis relative to the library used to develop lipid identifications.[55] For both TRAAK and TREK2, we observed several trends over sequential CV washes that pertained to the respective class of each lipid. Namely, PC and TG lipids were continually over-represented in TRAAK, while classes including SM, FFA, PS, and PE P- were uniquely high in specific CV wash steps. Conversely, TREK2 showed few preferential head groups except for PS lipids in early wash steps and TG, FFA, SM, PC, and PE P- in the later CVs. Previously, TRAAK displays a lack of specificity to PS acyl chains. Here, a mix of unsaturated and saturated PS species is identified across multiple wash steps.[33] While TG and plasmalogen PE species are not actively emphasized for their role in cell membranes, both classes have a presence in cellular membranes and are linked to increased membrane fluidity due to increased curvature.[69–71] We also note a possibility of lipid–lipid interactions that may be influencing the retention of these lipids. Fatty acyl enrichments also exhibited several trends including a significant bias of acyl composition of TREK2 enrichment compared to TRAAK. While both proteins showed enrichment of saturated fatty acids in later wash steps, TREK2 enrichment was initially characterized by 20 : 4 and 18 : 1-containing lipids. Arachidonic acid (20 : 4) is known to stimulate both TRAAK and TREK2.[72,73] These results show that indeed membrane proteins can enrich specific lipids from complex, natural extracts.

TREK channels are known to be stimulated by fatty acids and lysolipids.[57,74–76] Here, we found enrichment of fatty acids and lysolipids across the different wash steps. Regardless of the CV wash, TREK2 consistently enriched LPG(18 : 1), a lipid known to stimulate the channel.[74–76] Additionally, it should also be noted that for both TRAAK and TREK2, we observed a heightened enrichment of FFA. Both channels are known to be stimulated by FFAs.[57,77] While lipidomics identifies the retention of FFAs, intact masses measured by native MS do not show strong signals for bound FFA that could be the result of dissociation of these hydrophobically-bound molecules. In short, TRAAK and TREK2 can retain specific lipid species that are known to stimulate activity.

In summary, we describe an approach using immobilized membrane proteins to examine lipid binding from natural headgroup extracts and more complex lipid extracts, such as BEP. The use of natural headgroup extracts can be useful to discern how acyl chain chemistry impacts the binding of specific lipid types to the protein. As shown above, for TRAAK and TREK2, membrane proteins can enrich lipids from complex, natural lipid sources. In some cases, we observed the enrichment of lipids known to regulate TRAAK and TREK2. While the complexity of membrane protein–lipid interactions requires extensive validation to verify specificity, the results presented in this work demonstrate the approach will be useful for identifying lipids that regulate other membrane proteins. It is unclear the driving factor(s) for the selective enrichment of

lipid classes across CV wash steps and warrants further study. Another contributing factor can be the influence of lipid-protein interactions that in turn influence interaction with other lipids. For example, the presence of PE enhances AmtB–CDL interactions. While we focus here on commercially available lipid extracts, a future direction is the use of tissue- and/or membrane/organelle-specific lipid extracts, *e.g.* a plasma membrane lipid extract for a target membrane protein that resides in the plasma membrane. Thus, the combination of native MS and lipidomics provides a new means to better understand how the lipid environment modulates the structure and function of membrane proteins.

Data availability

Raw data and Skyline documents for lipidomic analysis are available at: **https://panoramaweb.org/PL_AL_EB_Lipidomics.url**.

Author contributions

YZ, MO, PQ, ESB and AL designed the research. YZ, PQ, TZ, and SS expressed and purified the membrane proteins. YZ, MO, and PQ performed mass spectrometry experiments. MO and ESB carried out the lipidomic studies. All authors analyzed the data. YZ, MO, PQ, ESB, and AL wrote the manuscript with input from the other authors.

Conflicts of interest

The authors declare no competing interests.

Acknowledgements

This work was supported by the National Institute of General Medical Sciences of the National Institutes of Health awarded (R01 GM121751 and R01 GM138863 to AL, R35 GM128624 to MTM, R01 DK122784 to MZ, R01 GM141277 to ESB, and RM1 GM145416 to AL, MZ, ESB, and MTM).

References

1 A. Laganowsky, et al., Membrane proteins bind lipids selectively to modulate their structure and function, *Nature*, 2014, **510**, 172–175, DOI: **10.1038/nature13419**.
2 A. G. Lee, Biological membranes: the importance of molecular detail, *Trends Biochem. Sci.*, 2011, **36**, 493–500, DOI: **10.1016/j.tibs.2011.06.007**.
3 F. X. Contreras, A. M. Ernst, F. Wieland and B. Brugger, Specificity of intramembrane protein–lipid interactions, *Cold Spring Harbor Perspect. Biol.*, 2011, **3**, a004705, DOI: **10.1101/cshperspect.a004705**.
4 M. Bogdanov, W. Dowhan and H. Vitrac, Lipids and topological rules governing membrane protein assembly, *Biochim. Biophys. Acta*, 2014, **1843**, 1475–1488, DOI: **10.1016/j.bbamcr.2013.12.007**.
5 S. J. Singer and G. L. Nicolson, The fluid mosaic model of the structure of cell membranes, *Science*, 1972, **175**, 720–731.
6 J. A. Poveda, et al., Lipid modulation of ion channels through specific binding sites, *Biochim. Biophys. Acta*, 2014, **1838**, 1560–1567, DOI: **10.1016/j.bbamem.2013.10.023**.
7 Q. X. Jiang and T. Gonen, The influence of lipids on voltage-gated ion channels, *Curr. Opin. Struct. Biol.*, 2012, **22**, 529–536, DOI: **10.1016/j.sbi.2012.03.009**.
8 J. E. Baenziger, C. M. Henault, J. P. Therien and J. Sun, Nicotinic acetylcholine receptor-lipid interactions: Mechanistic insight and biological function, *Biochim. Biophys. Acta*, 2015, **1848**, 1806–1817, DOI: **10.1016/j.bbamem.2015.03.010**.
9 M. Criado, H. Eibl and F. J. Barrantes, Effects of lipids on acetylcholine receptor. Essential need of cholesterol for maintenance of agonist-induced state transitions in lipid vesicles, *Biochemistry*, 1982, **21**, 3622–3629.
10 T. M. Fong and M. G. McNamee, Correlation between acetylcholine receptor function and structural properties of membranes, *Biochemistry*, 1986, **25**, 830–840.
11 F. I. Valiyaveetil, Y. Zhou and R. MacKinnon, Lipids in the structure, folding, and function of the KcsA K+ channel, *Biochemistry*, 2002, **41**, 10771–10777, DOI: **10.1021/bi026215y**.
12 S. McLaughlin and D. Murray, Plasma membrane phosphoinositide organization by protein electrostatics, *Nature*, 2005, **438**, 605–611, DOI: **10.1038/nature04398**.
13 C. L. Huang, S. Feng and D. W. Hilgemann, Direct activation of inward rectifier potassium channels by PIP2 and its stabilization by Gbetagamma, *Nature*, 1998, **391**, 803–806, DOI: **10.1038/35882**.
14 T. Rohacs, et al., Specificity of activation by phosphoinositides determines lipid regulation of Kir channels, *Proc. Natl. Acad. Sci. U. S. A.*, 2003, **100**, 745–750, DOI: **10.1073/pnas.0236364100**.
15 Y. Fujiwara and Y. Kubo, Regulation of the desensitization and ion selectivity of ATP-gated P2X2 channels by phosphoinositides, *J. Physiol.*, 2006, **576**, 135–149, DOI: **10.1113/jphysiol.2006.115246**.
16 S. B. Hansen, X. Tao and R. MacKinnon, Structural basis of PIP2 activation of the classical inward rectifier K+ channel Kir2.2, *Nature*, 2011, **477**, 495–498, DOI: **10.1038/nature10370**.
17 J. E. Keener, G. Zhang and M. T. Marty, Native Mass Spectrometry of Membrane Proteins, *Anal. Chem.*, 2021, **93**, 583–597, DOI: **10.1021/acs.analchem.0c04342**.
18 A. Laganowsky, E. Reading, J. T. Hopper and C. V. Robinson, Mass spectrometry of intact membrane protein complexes, *Nat. Protoc.*, 2013, **8**, 639–651, DOI: **10.1038/nprot.2013.024**.
19 N. P. Barrera, N. Di Bartolo, P. J. Booth and C. V. Robinson, Micelles protect membrane complexes from solution to vacuum, *Science*, 2008, **321**, 243–246, DOI: **10.1126/science.1159292**.
20 J. R. Bolla, M. T. Agasid, S. Mehmood and C. V. Robinson, Membrane Protein–Lipid Interactions Probed Using Mass Spectrometry, *Annu. Rev. Biochem.*, 2019, **88**, 85–111, DOI: **10.1146/annurev-biochem-013118-111508**.

21 T. M. Allison, et al., Quantifying the stabilizing effects of protein–ligand interactions in the gas phase, *Nat. Commun.*, 2015, **6**, 8551, DOI: 10.1038/ncomms9551.
22 S. M. Fantin, et al., Collision Induced Unfolding Classifies Ligands Bound to the Integral Membrane Translocator Protein, *Anal. Chem.*, 2019, **91**, 15469–15476, DOI: 10.1021/acs.analchem.9b03208.
23 X. Cong, Y. Liu, W. Liu, X. Liang and A. Laganowsky, Allosteric modulation of protein–protein interactions by individual lipid binding events, *Nat. Commun.*, 2017, **8**, 2203, DOI: 10.1038/s41467-017-02397-0.
24 H. Y. Yen, et al., PtdIns(4,5)P2 stabilizes active states of GPCRs and enhances selectivity of G-protein coupling, *Nature*, 2018, **559**, 423–427, DOI: 10.1038/s41586-018-0325-6.
25 J. W. Patrick, et al., Allostery revealed within lipid binding events to membrane proteins, *Proc. Natl. Acad. Sci. U. S. A.*, 2018, **115**, 2976–2981, DOI: 10.1073/pnas.1719813115.
26 J. Gault, et al., High-resolution mass spectrometry of small molecules bound to membrane proteins, *Nat. Methods*, 2016, **13**, 333–336, DOI: 10.1038/nmeth.3771.
27 J. Marcoux, et al., Mass spectrometry reveals synergistic effects of nucleotides, lipids, and drugs binding to a multidrug resistance efflux pump, *Proc. Natl. Acad. Sci. U. S. A.*, 2013, **110**, 9704–9709, DOI: 10.1073/pnas.1303888110.
28 H. Y. Yen, et al., Ligand binding to a G protein-coupled receptor captured in a mass spectrometer, *Sci. Adv.*, 2017, **3**, e1701016, DOI: 10.1126/sciadv.1701016.
29 J. R. Bolla, et al., Direct observation of the influence of cardiolipin and antibiotics on lipid II binding to MurJ, *Nat. Chem.*, 2018, **10**, 363–371, DOI: 10.1038/nchem.2919.
30 J. Marcoux and C. V. Robinson, Twenty years of gas phase structural biology, *Structure*, 2013, **21**, 1541–1550, DOI: 10.1016/j.str.2013.08.002.
31 J. Lyu, et al., Structural basis for lipid and copper regulation of the ABC transporter MsbA, *Nat. Commun.*, 2022, **13**, 7291, DOI: 10.1038/s41467-022-34905-2.
32 R. K. Saini, P. Prasad, X. Shang and Y. S. Keum, Advances in Lipid Extraction Methods-A Review, *Int. J. Mol. Sci.*, 2021, **22**, 13643, DOI: 10.3390/ijms222413643.
33 Y. Zhu, et al., Cupric Ions Selectively Modulate TRAAK–Phosphatidylserine Interactions, *J. Am. Chem. Soc.*, 2022, **144**, 7048–7053, DOI: 10.1021/jacs.2c00612.
34 H. Ilgü, et al., Variation of the detergent-binding capacity and phospholipid content of membrane proteins when purified in different detergents, *Biophys. J.*, 2014, **106**, 1660–1670, DOI: 10.1016/j.bpj.2014.02.024.
35 A. C. K. Teo, et al., Analysis of SMALP co-extracted phospholipids shows distinct membrane environments for three classes of bacterial membrane protein, *Sci. Rep.*, 2019, **9**, 1813, DOI: 10.1038/s41598-018-37962-0.
36 K. S. Simon, N. L. Pollock and S. C. Lee, Membrane protein nanoparticles: the shape of things to come, *Biochem. Soc. Trans.*, 2018, **46**, 1495–1504, DOI: 10.1042/bst20180139.
37 E. Reading, et al., Interrogating Membrane Protein Conformational Dynamics within Native Lipid Compositions, *Angew. Chem., Int. Ed.*, 2017, **56**, 15654–15657, DOI: 10.1002/anie.201709657.
38 K. A. Morrison, et al., Membrane protein extraction and purification using styrene–maleic acid (SMA) copolymer: effect of variations in polymer structure, *Biochem. J.*, 2016, **473**, 4349–4360, DOI: 10.1042/bcj20160723.
39 M. Barniol-Xicota and S. H. L. Verhelst, Lipidomic and in-gel analysis of maleic acid co-polymer nanodiscs reveals differences in composition of solubilized membranes, *Commun. Biol.*, 2021, **4**, 218, DOI: 10.1038/s42003-021-01711-3.
40 A. Laganowsky, et al., Membrane proteins bind lipids selectively to modulate their structure and function, *Nature*, 2014, **510**, 172–175, DOI: 10.1038/nature13419.
41 J. Lyu, et al., Discovery of Potent Charge-Reducing Molecules for Native Ion Mobility Mass Spectrometry Studies, *Anal. Chem.*, 2020, **92**, 11242–11249, DOI: 10.1021/acs.analchem.0c01826.
42 S. Schrecke, et al., Selective regulation of human TRAAK channels by biologically active phospholipids, *Nat. Chem. Biol.*, 2021, **17**, 89–95, DOI: 10.1038/s41589-020-00659-5.
43 M. T. Marty, et al., Bayesian Deconvolution of Mass and Ion Mobility Spectra: From Binary Interactions to Polydisperse Ensembles, *Anal. Chem.*, 2015, **87**, 4370–4376, DOI: 10.1021/acs.analchem.5b00140.
44 M. Bern, et al., Parsimonious Charge Deconvolution for Native Mass Spectrometry, *J. Proteome Res.*, 2018, **17**, 1216–1226, DOI: 10.1021/acs.jproteome.7b00839.
45 M. T. Marty, Fundamentals: How Do We Calculate Mass, Error, and Uncertainty in Native Mass Spectrometry?, *J. Am. Soc. Mass Spectrom.*, 2022, **33**, 1807–1812, DOI: 10.1021/jasms.2c00218.
46 E. S. Baker, K. Tang, W. F. Danielson, D. C. Prior and R. D. Smith, Simultaneous fragmentation of multiple ions using IMS drift time dependent collision energies, *J. Am. Soc. Mass Spectrom.*, 2008, **19**, 411–419, DOI: 10.1016/j.jasms.2007.11.018.
47 C. Becker, et al., A novel approach to collision-induced dissociation (CID) for ion mobility-mass spectrometry experiments, *J. Am. Soc. Mass Spectrom.*, 2009, **20**, 907–914, DOI: 10.1016/j.jasms.2008.11.026.
48 K. I. Kirkwood, et al., Utilizing Skyline to analyze lipidomics data containing liquid chromatography, ion mobility spectrometry and mass spectrometry dimensions, *Nat. Protoc.*, 2022, **17**, 2415–2430, DOI: 10.1038/s41596-022-00714-6.
49 B. X. MacLean, et al., Using Skyline to Analyze Data-Containing Liquid Chromatography, Ion Mobility Spectrometry, and Mass Spectrometry Dimensions, *J. Am. Soc. Mass Spectrom.*, 2018, **29**, 2182–2188, DOI: 10.1007/s13361-018-2028-5.
50 K. J. Adams, et al., Skyline for Small Molecules: A Unifying Software Package for Quantitative Metabolomics, *J. Proteome Res.*, 2020, **19**, 1447–1458, DOI: 10.1021/acs.jproteome.9b00640.
51 M. T. Odenkirk, B. M. Horman, J. N. Dodds, H. B. Patisaul and E. S. Baker, Combining Micropunch Histology and Multidimensional Lipidomic Measurements for In-Depth

Tissue Mapping, *ACS Meas. Sci. Au*, 2022, **2**, 67–75, DOI: 10.1021/acsmeasuresciau.1c00035.

52 K. I. Kirkwood, et al., Development and Application of Multidimensional Lipid Libraries to Investigate Lipidomic Dysregulation Related to Smoke Inhalation Injury Severity, *J. Proteome Res.*, 2022, **21**, 232–242, DOI: 10.1021/acs.jproteome.1c00820.

53 B. Peng, et al., LipidCreator workbench to probe the lipidomic landscape, *Nat. Commun.*, 2020, **11**, 2057, DOI: 10.1038/s41467-020-15960-z.

54 M. T. Odenkirk, et al., Structural-based connectivity and omic phenotype evaluations (SCOPE): a cheminformatics toolbox for investigating lipidomic changes in complex systems, *Analyst*, 2020, **145**, 7197–7209, DOI: 10.1039/d0an01638a.

55 G. Clair, et al., Lipid Mini-On: mining and ontology tool for enrichment analysis of lipidomic data, *Bioinformatics*, 2019, **35**, 4507–4508, DOI: 10.1093/bioinformatics/btz250.

56 A. G. Atanasov, S. B. Zotchev, V. M. Dirsch, T. International Natural Product Sciences and C. T. Supuran, Natural products in drug discovery: advances and opportunities, *Nat. Rev. Drug Discovery*, 2021, **20**, 200–216, DOI: 10.1038/s41573-020-00114-z.

57 M. Fink, et al., A neuronal two P domain K+ channel stimulated by arachidonic acid and polyunsaturated fatty acids, *EMBO J.*, 1998, **17**, 3297–3308, DOI: 10.1093/emboj/17.12.3297.

58 J. Noel, G. Sandoz and F. Lesage, Molecular regulations governing TREK and TRAAK channel functions, *Channels*, 2011, **5**, 402–409, DOI: 10.4161/chan.5.5.16469.

59 S. G. Brohawn, et al., The mechanosensitive ion channel TRAAK is localized to the mammalian node of Ranvier, *eLife*, 2019, **8**, e50403, DOI: 10.7554/eLife.50403.

60 T. Schmidt and A. Skerra, The Strep-tag system for one-step affinity purification of proteins from mammalian cell culture, *Methods Mol. Biol.*, 2015, **1286**, 83–95, DOI: 10.1007/978-1-4939-2447-9_8.

61 M. Sud, et al., LMSD: LIPID MAPS structure database, *Nucleic Acids Res.*, 2006, **35**, D527–D532, DOI: 10.1093/nar/gkl838.

62 H. Bang, Y. Kim and D. Kim, TREK-2, a new member of the mechanosensitive tandem-pore K+ channel family, *J. Biol. Chem.*, 2000, **275**, 17412–17419, DOI: 10.1074/jbc.M000445200.

63 J. Chemin, et al., Up- and down-regulation of the mechano-gated K(2P) channel TREK-1 by PIP (2) and other membrane phospholipids, *Pflugers Arch.*, 2007, **455**, 97–103, DOI: 10.1007/s00424-007-0250-2.

64 C. Cabanos, M. Wang, X. Han and S. B. Hansen, A Soluble Fluorescent Binding Assay Reveals PIP2 Antagonism of TREK-1 Channels, *Cell Rep.*, 2017, **20**, 1287–1294, DOI: 10.1016/j.celrep.2017.07.034.

65 H. Raghuraman and A. Chattopadhyay, Influence of lipid chain unsaturation on membrane-bound melittin: a fluorescence approach, *Biochim. Biophys. Acta*, 2004, **1665**, 29–39, DOI: 10.1016/j.bbamem.2004.06.008.

66 S. E. Feller, K. Gawrisch and A. D. MacKerell, Polyunsaturated Fatty Acids in Lipid Bilayers: Intrinsic and Environmental Contributions to Their Unique Physical Properties, *J. Am. Chem. Soc.*, 2002, **124**, 318–326, DOI: 10.1021/ja0118340.

67 S. Schrecke, et al., Selective regulation of human TRAAK channels by biologically active phospholipids, *Nat. Chem. Biol.*, 2021, **17**, 89–95, DOI: 10.1038/s41589-020-00659-5.

68 E. Fahy, et al., Update of the LIPID MAPS comprehensive classification system for lipids, *J. Lipid Res.*, 2009, **50**, S9–S14, DOI: 10.1194/jlr.R800095-JLR200.

69 J. Prades, S. S. Funari, P. V. Escribá and F. Barceló, Effects of unsaturated fatty acids and triacylglycerols on phosphatidylethanolamine membrane structure, *J. Lipid Res.*, 2003, **44**, 1720–1727, DOI: 10.1194/jlr.M300092-JLR200.

70 H. Khandelia, L. Duelund, K. I. Pakkanen and J. H. Ipsen, Triglyceride blisters in lipid bilayers: implications for lipid droplet biogenesis and the mobile lipid signal in cancer cell membranes, *PLoS One*, 2010, **5**, e12811, DOI: 10.1371/journal.pone.0012811.

71 Z. A. Almsherqi, Potential Role of Plasmalogens in the Modulation of Biomembrane Morphology, *Front. Cell Dev. Biol.*, 2021, **9**, 673917, DOI: 10.3389/fcell.2021.673917.

72 R. Ma and A. Lewis, Spadin Selectively Antagonizes Arachidonic Acid Activation of TREK-1 Channels, *Front. Pharmacol.*, 2020, **11**, 434, DOI: 10.3389/fphar.2020.00434.

73 S. Feliciangeli, F. C. Chatelain, D. Bichet and F. Lesage, The family of K2P channels: salient structural and functional properties, *J. Physiol.*, 2015, **593**, 2587–2603, DOI: 10.1113/jphysiol.2014.287268.

74 J. Chemin, et al., Lysophosphatidic acid-operated K+ channels, *J. Biol. Chem.*, 2005, **280**, 4415–4421, DOI: 10.1074/jbc.M408246200.

75 R. Juarez-Contreras, T. Rosenbaum and S. L. Morales-Lazaro, Lysophosphatidic Acid and Ion Channels as Molecular Mediators of Pain, *Front. Mol. Neurosci.*, 2018, **11**, 462, DOI: 10.3389/fnmol.2018.00462.

76 F. Maingret, A. J. Patel, F. Lesage, M. Lazdunski and E. Honore, Lysophospholipids open the two-pore domain mechano-gated K(+) channels TREK-1 and TRAAK, *J. Biol. Chem.*, 2000, **275**, 10128–10133, DOI: 10.1074/jbc.275.14.10128.

77 N. Smithers, J. H. Bolivar, A. G. Lee and J. M. East, Characterizing the Fatty Acid Binding Site in the Cavity of Potassium Channel KcsA, *Biochemistry*, 2012, **51**, 7996–8002, DOI: 10.1021/bi3009196.